

Maximum entropy and population heterogeneity in continuous cell cultures meet experimental data, preliminary results

September 26, 2019

1 Materials and Method

1.1 Model framework

The model framework used is detaily explained in (Fernandez-de Cossio-Diaz, Leon, & Mulet, 2017) and (Fernandez-de Cossio-Diaz & Mulet, 2019).

1.2 Experimental data

Experimental data were taken from (Rath, 2017). In this work, the author performed 6 continuous cultures, (A, B, C, D, E, F), with the cell line AGE1.HN.AA1. The parental line AGE1.HN was established by the company ProBioGen (ProBioGen AG, Berlin, Germany) from a tissue sample of a human brain. All culture's feed mediums were based on the standard 42-Max-UB-medium, which is serum-free and was specially developed for the AGE1.HN cell line *Table 1*. The experiments were run under various conditions, differing mainly in the dilution rate (D) and the feed medium composition of glucose (GLC), glutamine (GLN) and galactose ($GAL/GALC$) *Table 2*.

For each experiment, a steady-state condition was reached, ($A, B, C, D, E, F01$), and several observables was reported *Tables 3 – 4*. Particularly relevant for this work was the growth rate (μ), D , the viable cell density (Xv) and the medium concentration (s) and derived uptake rate (u) for a set of metabolites (GLC , lactose (LAC), GLN , ammonium (NH_4), GAL , pyruvate (PYR), glutamate (GLU), alanine (ALA), asparagine (ASP)). A unit conversion was required to make experimental data and our model compatible. For this propose the only external data needed was the cell mass density. It was used $0.25 \text{ pgDW} / \mu\text{m}^3$ (Niklas, Schröder, Sandig, Noll, & Heinzle, 2011). ;

2 Results

2.1 Low concentrations of phosphatidylethanolamine

Because phosphatidylethanolamine isn't a reported component of the 42-Max-UB-medium, *Tabla 1*, and it can be a carbon source for the GEMs, its concentration was set first to the lowest value possible. For Recon3D it was fixed to 0.1mM, a handpicked value, and for CHO it wasn't present in the feed medium at all.

Flux balance analysis with molecular crowding (FBA) was performed similarly to (Fernandez-de Cossio-Diaz & Mulet, 2019). Plots of μ and Xv as a function of ξ are shown in *Figure 1*. Both networks failed to reach the experimental values for both observables. In the case of Xv , in all the explored ξ range (from 1 to 1000 gDW hr/ L) the value was underestimated. This result may have several causes. One could be that the GEM has a "too expensive" biomass equation. We mean that one or more biomass required precursors might be overestimated. However, this reason seems hard to sustain because we modified the Recon3D biomass equation with the reported anabolic biomass demand for AGE1.HN.AA1 (Niklas, Priesnitz, Rose, Sandig, & Heinzle, 2013). We use the reported anabolic demand of proteins, lipids, DNA, RNA, and carbohydrates to fix the total demand of these same groups in the original Recon3D biomass equation and the changes weren't too big. For CHO we kept the biomass equation unmodified. Nonetheless, a modification in the biomass equation would be an elegant way to solve the problem. Another plausible cause could be a big difference between the model's frameworks. But, both works model the chemostat in an equivalent fashion, as can be seen when comparing equations 1 with 3.25 and 2 with 3.28 and 3.29 from (Fernandez-de Cossio-Diaz et al., 2017) and (Rath, 2017) respectively.

Moreover, other parameter than can affect Xv is the bleeding coefficient, ϕ , defined in perfusion systems as the fraction of cells that escape from the culture through a cell-retention device (Fernandez-de Cossio-Diaz et al., 2017). Because, (Rath, 2017) doesn't report the use of any retention device in the cultures this parameter was taken as 1.0, but lower values will cause to increment the predicted value of Xv by the model. Finally, it needs to be taken into consideration that we are using GEMs that are not directed curated for the working cell line. In fact, a crucial phenotypic feature reported for AGE1.HN.AA1 like the impossibility of growth in GLN free mediums (Rath, 2017) is not reproduced by the used GEMs. This is, by far, the most difficult factor to solve, because the curation of a genome-scale metabolic network is a very laborious process.

On the other hand, correlations of experimental and modeled uptakes, *Figure 2*, were performed. The graphs show better results for the uptakes of *GLC* and *GLN*, and worse correlations for uptakes such as *PYR*, *NH4* and *LAC* for both GEMs. In general, CHO had better correlations than Recon3D. This could be, maybe, explained because Recon3D is a general GEM, allowing the model to access to all the possible genome repertory present in humans, a fact that is not accurate for a cell in the *in vivo* scenario. Additionally, CHO was curated for

a defined cell line, representing a more restricted and realistic network. Anyway, it is remarkable that the models reproduce uptakes like *GLC* and *GLN* regarding all the previous consideration.

2.2 High concentrations of phosphatidylethanolamine

To avoid the undesired Xv and μ underestimation, a less realistic scenario was considered. An extra carbon source was put in excess in the feed medium. We select the phosphatidylethanolamine (*PE*) because it was already introduced in the Recon3D medium, do to the incapacity of this GEM to growth without this (or similar) metabolite, and it is an usable carbon source. So, the feed medium concentration of *PE* was set to a high value, 20 mM (handpicked value), for both GEMs.

This time, additionally to *FBA*, the expected propagation (*EP*) algorithm was used to introduce a population heterogeneity factor (Fernandez-de Cossio-Diaz & Mulet, 2019). *Figure 3* shows the results of both methods for Recon3D and CHO. As can be appreciated, *FBA* (Blue solid line) overestimate the experimental results. This is consistent with the fact that we put a carbon source, *PE*, in a high concentration, allowing the network to reach higher μ and Xv values.

On the other hand, *EP* can be tuned through parameter β . This parameter can be interpreted as a measurement of the cell heterogeneity in the culture (Fernandez-de Cossio-Diaz & Mulet, 2019). β values closer to zero indicate higher heterogeneity in the culture, or that the cells can explore more uniformly the space of possibles metabolic states. By contrast, larger β values will be approaching the *EP* model result to *FBA* result, meaning that no cell heterogeneity is accounted at all. As is appreciated in *Figure 3*, considering different β values allow the *EP* model to reproduce the measured μ and Xv . This is an interesting result for several reasons. First, it improves the *FBA* solution. *FBA* is insensible to the different experimental conditions, as shown in *Figure 1 and 3*. This means that it does not vary the observable predictions, mainly Xv , after changing the particular culture conditions, metabolite feed medium concentrations and dilution rate. This occurs for both situations, low and high concentration of *PE*, at least with this *GEMs* and settings. This could, maybe, be explained because *FBA*, as used in this work, returns an optimal metabolic state that maximizes μ . However, it is possible that many different states maximize μ , a not unique solution scenario, and this can make the network robust enough to be insensible to the changes in the input.

Because *EP* introduces the heterogeneity factor, a better exploration of the space of feasible metabolic states is now possible. There are many factors that can influence the heterogeneity of a population of cells "SacarcitasdeCossio2019pag3". The observable results can be then interpreted, not only because different input conditions lead to a unique different metabolic state, but because these same changes in the input modified the likelihood distribution of the feasible metabolic states through the cell population. This interpretation is qualitatively different from what *FBA* represents.

Furthermore, the correlation of experimental and modeled uptakes was performed, *Figure 4*, for both methods. Again, the best correlations were achieved for the uptakes of *GLC* and *GLN*. A small improvement in the general results can be observed for *EP* compared with *FBA*, in particular for Recon3D. The causes that are driven by these results could be the same disused in the previous section.

3 References

Fernandez-de Cossio-Diaz, J., Leon, K., & Mulet, R. (2017). Characterizing steady states of genome-scale metabolic networks in continuous cell cultures. *PLoS Computational Biology*, 13(11), 1–22. doi: 10.1371/journal.pcbi.1005835

Fernandez-de Cossio-Diaz, J., & Mulet, R. (2019). Maximum entropy and population heterogeneity in continuous cell cultures. *PLoS Computational Biology*, 15(2). Retrieved from <http://arxiv.org/abs/1807.03982> doi: 10.1371/journal.pcbi.1006823

Niklas, J., Priesnitz, C., Rose, T., Sandig, V., & Heinzle, E. (2013). Metabolism and metabolic burden by a 1 -antitrypsin production. *Metabolic Engineering*, 16, 103–114. Retrieved from <http://dx.doi.org/10.1016/j.ymben.2013.01.002> doi: 10.1016/j.ymben.2013.01.002

Niklas, J., Schröder, E., Sandig, V., Noll, T., & Heinzle, E. (2011). Quantitative characterization of metabolism and metabolic shifts during growth of the new human cell line AGE1.HN using time resolved metabolic flux analysis. *Bioprocess and Biosystems Engineering*, 34(5), 533–545. doi: 10.1007/s00449-010-0502-y

Rath, A. (2017). *Characterisation of cell growth, metabolism and recombinant protein production during transient and steady state conditions for the human cell line AGE1.HN-AAT* (Doctoral dissertation). Retrieved from https://pure.mpg.de/pubman/item/item_2508673_4

4 Tables and Figures

Substance	Value	Dimension	Analytical method
Pluronic	1.0	g/L	as stated by Xell
NaHCO ₃	2.1	g/L	as stated by Xell
Osmolality	290.0	mOsm/kg	FPDO ^a
pH value	7.4	-	pH meter
GALC	0.5	g/L	AEC ^b
GLC	5.5	g/L	Bioprofile
AMM	0.3	mM	Bioprofile
LAC	0.0	g/L	Bioprofile
PYR	2.9	mM	AEC
GLU	636.9	μM	AEC
ALA	437.1	μM	AEC
ARG	1588.2	μM	AEC
ASN	920.4	μM	AEC
ASP	2197.9	μM	AEC
CYS	963.1	μM	AEC
GLY	1196.0	μM	AEC
HIS	642.7	μM	AEC
ILE	1744.9	μM	AEC
LEU	1893.2	μM	AEC
LYS	1256.0	μM	AEC
MET	601.3	μM	AEC
PHE	1039.4	μM	AEC
PRO	1040.5	μM	AEC
SER	3027.4	μM	AEC
THR	1502.4	μM	AEC
TRP	383.8	μM	AEC
TYR	1109.7	μM	AEC
VAL	1811.9	μM	AEC

a: freezing point depression osmometer (FPDO); b: anion exchanger chromatography (AEC);

Table 1: Measured medium composition of the 42-MAX-UB standard medium. Extracted from (Rath, 2017)

Exp. ID	<i>DR</i> (1/h)	Preculture (passage no.)	GLC (mM)	GLN (mM)	GALC (mM)
A	0.0140	7	10	5	3
B	0.0120	7	10	5	3
C	0.0100	5	10	5	3
D	0.0150	8	10	2	3
E	0.0133	4	8	2	3
F01	0.0150	10	10	5	0

Table 2: The dilution rates, preculture ages and the 42-Max-UB-medium modified components concentrations used in (Rath, 2017) for the 6 steady states. Table adapted from (Rath, 2017)

Variable	Exp. A		Exp. B		Exp. C		Exp. D		Exp. E	
	Average \pm SD	Rel. SD (%)	Average \pm SD	Rel. SD (%)	Average \pm SD	Rel. SD (%)	Average \pm SD	Rel. SD (%)	Average \pm SD	Rel. SD (%)
Setpoints:										
<i>DR</i> (h)	0.0140	-	0.0120	-	0.0100	-	0.0150	-	0.0133	-
GLC feed conc. (mM)	10.0	-	10.0	-	10.0	-	10.0	-	8.0	-
GLN feed conc. (mM)	5.0	-	5.0	-	2.0	-	2.0	-	2.0	-
GALC feed conc. (mM)	3.0	-	3.0	-	3.0	-	3.0	-	3.0	-
GLC/GLN ratio (mol/mol)	2	-	2	-	2	-	5	-	4	-
<i>X_V</i> (E6 cells/mL)	2.490 \pm 0.100	4.0	2.745 \pm 0.118	4.3	2.735 \pm 0.056	2.0	1.489 \pm 0.043	2.9	0.998 \pm 0.025	2.5
<i>X_D</i> (E6 cells/mL)	0.210 \pm 0.032	15.2	0.291 \pm 0.021	7.4	0.378 \pm 0.047	12.5	0.086 \pm 0.006	6.5	0.075 \pm 0.014	18.5
<i>CV_V</i> (μ L/mL)	6.56 \pm 0.48	7.4	7.19 \pm 0.67	9.4	6.23 \pm 0.21	3.4	4.33 \pm 0.27	6.3	3.40 \pm 0.17	4.9
μ (1/h)	0.0152 \pm 0.0002	1.2	0.0133 \pm 0.0001	1.1	0.0114 \pm 0.0002	1.4	0.0159 \pm 0.0001	0.6	0.0143 \pm 0.0002	1.4
<i>CD</i> (μ m)	17.1 \pm 0.25	1.5	17.2 \pm 0.19	1.1	16.3 \pm 0.24	1.5	17.7 \pm 0.30	1.5	18.7 \pm 0.20	1.1
GLC (mM)	0.0 \pm 0.00	-	0.0 \pm 0.00	-	0.0 \pm 0.00	-	0.0 \pm 0.00	-	0.0 \pm 0.00	-
LAC (mM)	2.1 \pm 1.52	-	0.5 \pm 0.02	3.5	0.6 \pm 0.04	7.3	12.5 \pm 0.60	5.0	12.7 \pm 0.40	3.0
GLN (mM)	0.8 \pm 0.08	10.0	5.5 \pm 0.19	3.5	5.9 \pm 0.09	1.5	0.5 \pm 0.10	11.1	0.5 \pm 0.10	13.7
AMM (mM)	3.4 \pm 0.22	6.7	1.9 \pm 0.06	2.9	1.7 \pm 0.02	0.9	1.5 \pm 0.03	2.1	1.6 \pm 0.02	1.6
GALC (mM)	1.9 \pm 0.08	4.5	1.9 \pm 0.06	2.9	1.7 \pm 0.02	0.9	2.1 \pm 0.10	2.5	2.4 \pm 0.10	3.2
PYR (mM)	0.2 \pm 0.00	1.8	0.1 \pm 0.00	3.2	0.1 \pm 0.00	3.2	0.3 \pm 0.04	12.6	1.1 \pm 0.10	5.3
GLU (mM)	1.2 \pm 0.08	6.2	1.3 \pm 0.01	0.5	1.0 \pm 0.05	5.0	0.7 \pm 0.10	12.9	0.8 \pm 0.10	12.8
ALA (mM)	1.4 \pm 0.09	6.4	0.2 \pm 0.03	13.8	0.1 \pm 0.01	14.2	0.3 \pm 0.02	8.9	1.0 \pm 0.05	5.2
ASP (mM)	1.6 \pm 0.06	3.9	1.5 \pm 0.05	3.2	1.3 \pm 0.02	1.2	2.4 \pm 0.17	7.1	2.8 \pm 0.30	10.8
ALAT (mg/L)	57.9 \pm 3.03	5.2	81.0 \pm 9.21	11.4	72.1 \pm 1.09	1.5	50.9 \pm 1.50	2.9	44.6 \pm 2.80	6.2
<i>Y_{CvV/glc}</i> (μ L/mmol)	711 \pm 47	6.6	827 \pm 77	9.4	753 \pm 17	2.3	482 \pm 30	6.3	518 \pm 18	3.5
<i>Y_{CvV/gln}</i> (μ L/mmol)	1679 \pm 140	8.3	1770 \pm 145	8.2	1601 \pm 52	3.3	3617 \pm 215	6.0	2837 \pm 201	7.1
<i>Y_{lac/glc}</i> (mol/mol)	0.2 \pm 0.15	-	0.0 \pm 0.01	-	0.0 \pm 0.00	-	1.2 \pm 0.10	5.3	1.8 \pm 0.10	3.2
<i>Y_{amm/glc}</i> (mol/mol)	0.8 \pm 0.05	6.6	1.2 \pm 0.04	3.6	1.3 \pm 0.03	1.9	1.0 \pm 0.05	4.9	1.1 \pm 0.10	4.8
<i>Y_{ala/gln}</i> (mol/mol)	0.2 \pm 0.02	9.5	0.0 \pm 0.00	-	0.0 \pm 0.00	-	0.0 \pm 0.00	-	0.6 \pm 0.04	7.9
<i>q_{GLC}</i> (mmol/gL h) ^a	21.43 \pm 1.56	7.3	16.17 \pm 1.76	10.9	15.13 \pm 0.51	3.4	33.05 \pm 2.17	6.6	27.64 \pm 1.33	4.8
<i>q_{LAC}</i> (mmol/gL h) ^a	-4.43 \pm 3.05	-	0.00 \pm 0.00	-	0.00 \pm 0.00	-	-41.23 \pm 4.13	10.0	-49.68 \pm 1.30	2.6
<i>q_{GLN}</i> (mmol/gL h) ^a	9.10 \pm 0.82	9.0	7.55 \pm 0.72	9.5	7.12 \pm 0.31	4.3	4.40 \pm 0.28	6.4	5.07 \pm 0.41	8.1
<i>q_{AMM}</i> (mmol/gL h) ^a	-7.19 \pm 0.67	9.3	-9.21 \pm 0.97	10.5	-9.55 \pm 0.30	3.2	-4.48 \pm 0.35	7.8	-5.66 \pm 0.33	5.9
<i>q_{PYR}</i> (mmol/gL h) ^a	1.94 \pm 0.21	10.8	1.55 \pm 0.22	14.3	2.46 \pm 1.26	51.1	1.92 \pm 0.24	12.3	1.61 \pm 0.37	23.3
<i>q_{PYR}</i> (mmol/gL h) ^a	5.82 \pm 0.52	8.9	4.70 \pm 0.57	12.1	4.48 \pm 0.11	2.4	9.10 \pm 0.64	7.1	7.04 \pm 0.55	7.8
<i>q_{GLU}</i> (mmol/gL h) ^a	-1.31 \pm 0.18	14.0	-1.05 \pm 0.10	9.4	-0.52 \pm 0.09	17.9	-0.71 \pm 0.31	43.5	-0.88 \pm 0.38	43.8
<i>q_{ALA}</i> (mmol/gL h) ^a	-2.14 \pm 0.27	12.8	0.39 \pm 0.03	6.7	0.54 \pm 0.03	5.9	0.10 \pm 0.12	127.8	-2.81 \pm 0.26	9.4
<i>q_{ASP}</i> (mmol/gL h) ^a	1.19 \pm 0.19	15.9	1.20 \pm 0.10	8.1	1.49 \pm 0.05	3.5	-0.41 \pm 0.62	150.7	-2.16 \pm 1.15	53.1
<i>q_{ALAT}</i> (mg/cell d) ^a	-7.87 \pm 0.19	2.4	-8.54 \pm 1.34	15.7	-6.33 \pm 0.19	3.0	-12.31 \pm 0.60	4.9	-14.29 \pm 1.08	7.5

^a: Substrate uptake is indicated by a positive rate, whereas a negative value indicates a production rate.

Table 3: Steady-state values reported by (Rath, 2017) for different parameters from continuous cultivations, varying GLC and GLN feed concentrations and with 3 mM GAL. Table taken from (Rath, 2017)

Variable	Exp. F01	
	Average \pm SD	Rel. SD (%)
Setpoints:		
<i>DR</i> (1/h)	0.0150	-
GLC feed conc. (mM)	10	-
GLN feed conc. (mM)	5	-
GALC feed conc. (mM)	0	-
GLC/GLN ratio (mol/mol)	2	-
X_V (E6 cells/mL)	1.701 ± 0.023	1.3
X_D (E6 cells/mL)	0.081 ± 0.004	5.1
CV_V (μ L/mL)	4.54 ± 0.24	5.2
μ (1/h)	0.0156 ± 0.0000	0.2
CD (μ m)	17.2 ± 0.33	1.9
GLC (mM)	0.0 ± 0.00	-
LAC (mM)	7.8 ± 0.64	8.2
GLN (mM)	1.9 ± 0.18	9.3
AMM (mM)	3.4 ± 0.17	5.1
PYR (mM)	0.4 ± 0.02	6.6
GLU (mM)	1.0 ± 0.05	5.2
ALA (mM)	0.9 ± 0.07	8.2
ASP (mM)	1.9 ± 0.21	10.8
AIAT (mg/L)	44.0 ± 1.71	3.9
$Y_{CVV/glc}$ (μ L/mmol)	626 ± 25	4.0
$Y_{CVV/gln}$ (μ L/mmol)	1865 ± 201	10.8
$Y_{lac/glc}$ (mol/mol)	0.9 ± 0.07	8.2
$Y_{amm/gln}$ (mol/mol)	1.3 ± 0.04	3.1
$Y_{ala/gln}$ (mol/mol)	0.2 ± 0.02	8.5
q_{GLC} (nmol/ μ L h) ^a	24.9 ± 1.08	4.3
q_{LAC} (nmol/ μ L h) ^a	-22.6 ± 1.27	5.6
q_{GLN} (nmol/ μ L h) ^a	8.4 ± 1.07	12.7
q_{AMM} (nmol/ μ L h) ^a	-10.9 ± 1.13	10.3
q_{PYR} (nmol/ μ L h) ^a	4.5 ± 0.31	6.9
q_{GLU} (nmol/ μ L h) ^a	-0.7 ± 0.15	20.4
q_{ALA} (nmol/ μ L h) ^a	-1.99 ± 0.33	16.3
q_{ASP} (nmol/ μ L h) ^a	1.65 ± 0.64	39.0
q_{AIAT} (pg/cell d) ^a	-9.2 ± 0.25	2.7

^a: Substrate uptake is indicated by a positive rate, whereas a negative value indicates a production rate.

Table 4: Steady-state values reported by (Rath, 2017) of different parameters from continuous cultivations, varying GLC and GLN feed concentrations and without GAL. Table taken from (Rath, 2017)

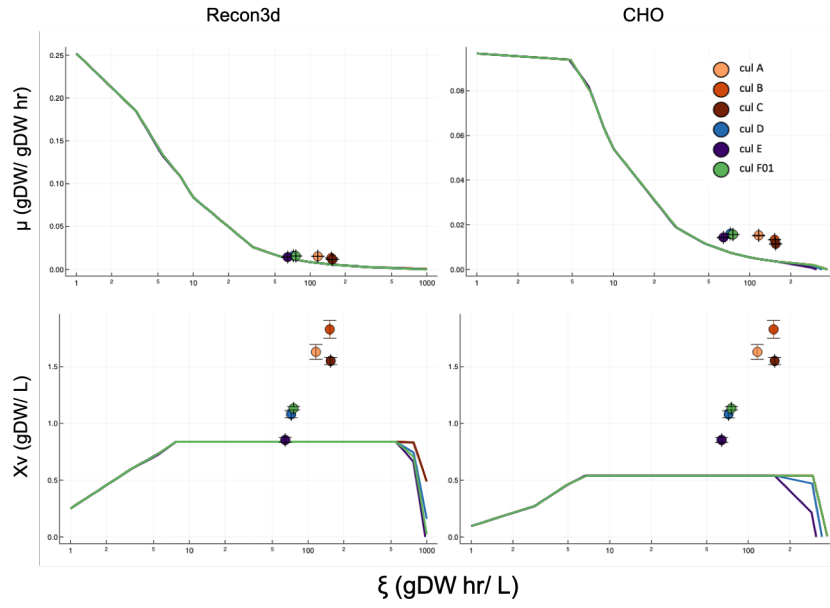


Figure 1: FBAwMC results showing the growth rate, μ , and the viable cell density, X_v , dependence of ξ for the six steady states. The solid lines represent the model predictions and the colored points show the experimental results. The model data was obtained for feed mediums with low (Recon3D) and zero (CHO) concentration of phosphatidylethanolamine

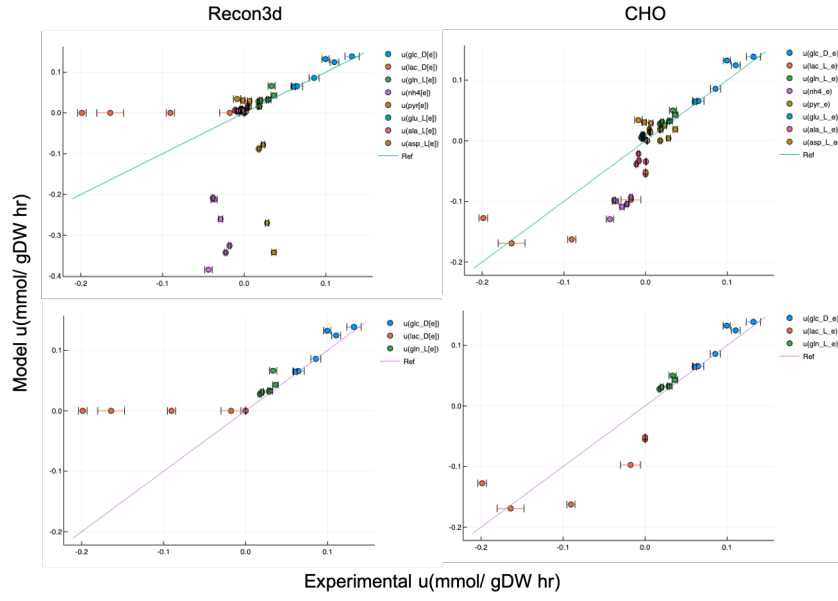


Figure 2: Correlations of all the experimental uptakes, upper graphs, and a selected subset, inferior graphs, respect to the predicted value from FBAwMC with low (Recon3D) and zero (CHO) concentration of phosphatidylethanolamine.

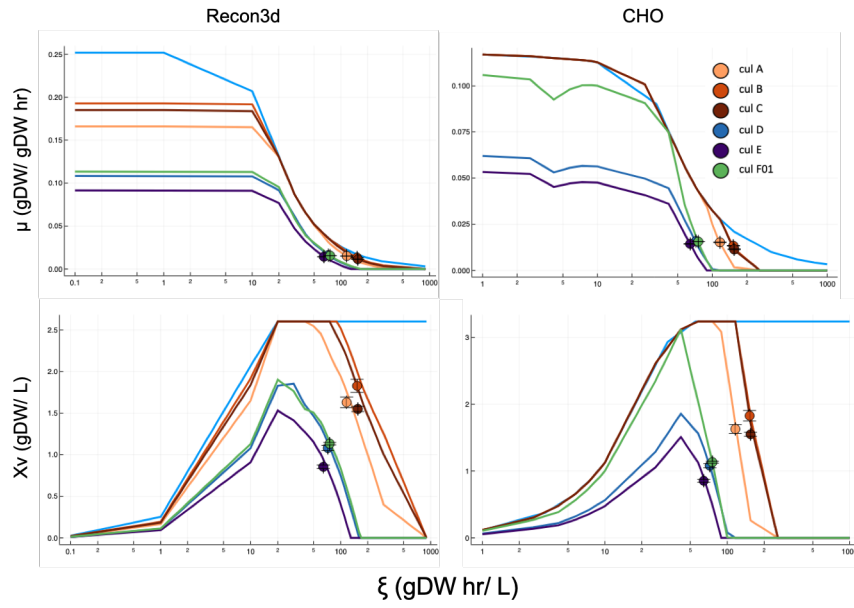


Figure 3: EP and FBA results showing the growth rate and the viable cell density dependence of ξ for the six culture conditions. The solid lines represent the model predictions and the color points show the experimental results. FBA results are shown as the solid light blue line. *EP* β parameters was chosen, for each culture, so that the experimental μ coincides with the predicted μ

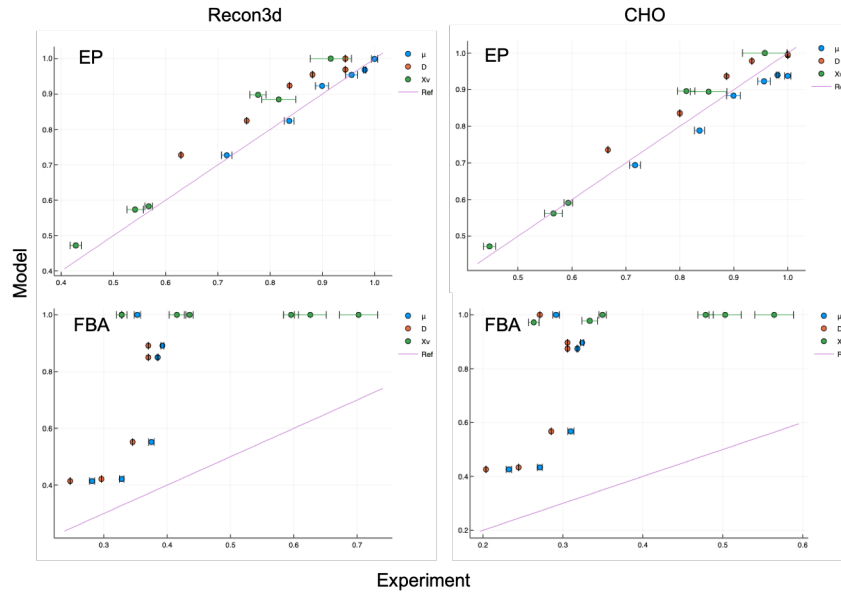


Figure 5: Normalized correlations of the experimental μ , D and Xv compared with the predicted value from EP and FBA for GEMs with high concentration of phosphatidylethanolamine.